Supplementary Information

Impedance microscopy for imaging solid-state battery interfaces

Yuji Yamagishi*, Hirotada Gamo, Zyun Siroma, Naoya Ishida, Yasushi Maeda, Tetsu Kiyobayashi, Nobuhiko Takeichi, Kentaro Kuratani, Hikaru Sano

Research Institute of Electrochemical Energy, Department of Energy and Environment, National Institute of Advanced Industrial Science and Technology (AIST), 1-8-31 Midorigaoka, Ikeda, Osaka 563-8577, Japan

*Corresponding Author: Y.Y. y.yamagishi@aist.go.jp

Table of contents

Supplementary Note 1

Principle and implementation of EIS-AFM

SIM visualizes the spatial distribution of AC potentials in a sample by measuring the amplitude and phase of the electrostatic force between a conductive probe and the sample. Early implementations of SIM employed an amplitude-modulation (AM) scheme for electrostatic force detection, which allows relatively high measurement frequencies[1,2]. However, this approach suffers from limited spatial resolution because the detected signal includes not only the electrostatic force between the probe apex and the sample but also parasitic contributions arising from the cantilever beam.

To suppress these non-local contributions, it is preferable to detect sideband components generated by the modulation of the probe vibration by the applied AC signal, rather than directly detecting the electrostatic force at the same frequency as the applied signal, as in the AM scheme (Supplementary Fig. 1). Based on this concept, frequency-modulation SIM (FM-SIM) was developed, which significantly improves spatial resolution[3]. In FM-SIM, a low-frequency AC signal (typically a few kHz) is applied to the sample, and the resulting sideband component appearing near the first resonance frequency of the cantilever is detected using an FM detector. This method selectively detects the localized electrostatic force at the probe apex.

Despite this advantage, the FM scheme imposes a limitation on the accessible measurement frequency. The frequency of the applied AC signal is constrained by the bandwidth of the FM detector, which typically allows detection only up to 5 kHz. As a result, SIM measurement at higher frequencies has remained difficult.

This limitation can be overcome by introducing a heterodyne detection scheme for electrostatic force measurements in SIM. The heterodyne approach enables detection of sideband components generated by high-frequency AC signals (>5 kHz) applied to the sample[4]. Because the signal of interest is still encoded in the sideband component of the first cantilever resonance as in the FM scheme, high spatial resolution is preserved while extending the accessible measurement frequency range (Supplementary Table 1). Furthermore, because the signal is detected at the second resonance frequency of the cantilever in the heterodyne scheme, the larger amplitude gain enables more sensitive detection than in the FM scheme.

In heterodyne electrostatic force detection, an AC signal whose frequency is determined by the cantilever resonance frequencies is applied to the sample. Specifically, the excitation frequency is set to the difference between the second and first resonance frequencies of the cantilever,

$$f_1 - f_0$$

(Supplementary Fig. 1).

However, SIM measurements require sweeping the sample excitation frequency over several orders of magnitude. Direct detection of this signal using the heterodyne scheme is therefore not feasible. To address this issue, the frequency of the sample AC signal is converted into a frequency compatible with heterodyne detection. In practice, an additional AC signal is applied to the probe for frequency conversion. The mixed-frequency component generated by the interaction between this signal and the sample excitation signal is tuned to match the frequency required for heterodyne detection (Details of the frequency configuration are described in Supplementary Note 2). This approach enables heterodyne electrostatic force detection to be implemented in broadband SIM measurements.

	AM-SIM	**FM-SIM**	**EIS-AFM**
Spatial resolution	Low	High	High
Upper frequency limit	High (440 kHz)	Low (5 kHz)	High (no fundamental limit)
Ref.	[1,2]	[3,5]	This work

Supplementary Table 1 | Characteristics of different SIM detection schemes. The upper frequency limit was calculated for a cantilever with a first resonance frequency of 70 kHz and a second resonance frequency of 440 kHz, assuming an FM detector bandwidth of 5 kHz.

Supplementary Note 2

Frequency configuration of EIS-AFM

As described in Supplementary Note 1, heterodyne detection is implemented in SIM by converting the sample AC signal into a frequency component that can be detected at the cantilever resonance. This section describes the detailed frequency configuration used in the measurements.

In the SIM measurements, a DC bias equal to the open-circuit voltage of the battery is applied to the sample, on which an AC signal at the measurement frequency f_s is superimposed. The probe is driven with three electrical components: an AC signal at frequency f_{t1} for KPFM, a DC feedback voltage, and an AC signal at frequency f_{t2} for SIM signal detection.

The SIM measurement determines the spatial distribution of the amplitude and phase of the AC potential at frequency f_s. In this work, the f_s component is detected indirectly through frequency mixing with the probe-applied signal at f_{t2}. The resulting mixed component is designed to match the difference between the second and first resonance frequencies of cantilever. For low measurement frequencies ($f_s < f_1 - f_0$), the sum-frequency component

$$f_s + f_{t2}$$

is tuned to equal the resonance difference

$$f_1 - f_0$$

giving

$$f_{t2} = f_1 - f_0 - f_s$$

For higher measurement frequencies ($f_s > f_1 - f_0$), the difference-frequency component

$$f_s - f_{t2}$$

is adjusted to match

$$f_1 - f_0$$

yielding

$$f_{t2} = f_s - f_1 + f_0$$

Under these conditions, the electrostatic force component carrying the f_s information appears at the second cantilever resonance f_1. This component is detected using a lock-in amplifier, allowing the amplitude and phase of the f_s signal to be extracted. This configuration enables broadband SIM measurements while maintaining nearly constant detection sensitivity, because the mixed-frequency component can always be aligned with the cantilever resonance by adjusting f_{t2}.

In addition to this configuration, referred to as the low-f modes, an alternative high-f mode is possible. In this case, the other difference-frequency component

$$f_{t2} - f_s$$

is matched to

$$f_1 - f_0$$

giving

$$f_{t2} = f_s + f_1 - f_0$$

The high-f mode does not require switching between frequency conditions depending on f_s. However, it requires significantly higher f_{t2} frequencies, which introduces high-frequency signals into the probe circuitry (Supplementary Fig. 2). For practical measurements, the low-f modes are therefore preferable. All measurements in this study were performed using the low-f modes configuration.

Simultaneous KPFM measurements were performed to improve the accuracy of the SIM measurements. In KPFM, the probe potential is feedback-controlled to match the local surface potential of the sample, thereby suppressing undesired electrostatic forces between the probe and sample. The KPFM measurement employs a conventional frequency-modulation scheme. An AC signal at frequency f_{t1} modulates the first cantilever resonance, and the resulting sideband signal is detected using an FM detector. The output is demodulated with a lock-in amplifier and used to adjust the DC bias applied to the probe, allowing the surface potential to be determined. Simultaneous SIM–KPFM measurements have been reported previously and therefore do not represent a methodological novelty in this work[3,5].

Supplementary Note 3

Measurement and analysis of partial impedance spectra of RC circuits using EIS-AFM

For the measurement of partial impedance spectra of RC circuits using EIS-AFM, a measurement setup employing Au electrodes was constructed, as shown in Fig. 4a. Using this setup, the partial impedances of an RC circuit consisting of resistors and a capacitor (Z_1 and Z_2) were extracted. The procedure for deriving the partial impedances is described below.

Measurement procedure

1. The frequency response of the SIM signal was measured on an Au electrode to which the AC excitation signal was directly applied (reference measurement).

2. The frequency responses of the SIM signal and the current were measured on an Au electrode connected to the intermediate node of the RC circuit (main measurement).

Calculation procedure

1. The total circuit impedance (Z_{all}) was calculated from the measured frequency responses of the applied AC signal and the current using the same procedure as in conventional EIS.

2. The frequency dependence of the AC potential at the intermediate node of the RC circuit was obtained by multiplying the applied AC signal by the frequency-dependent intensity ratio of the SIM signals obtained in the reference and main measurements. The partial impedance Z_1 was then calculated by dividing this result by the measured frequency response of the current.

3. The second partial impedance Z_2 was calculated by subtracting Z_1 from Z_{all}.

The measured frequency response of the current and the partial impedance spectra obtained using SIM are shown in Fig. 4 and Supplementary Fig. 7. Measurements were performed under two conditions with different cutoff frequencies of the RC circuit: a low cutoff frequency condition ($R_1 = 2\,\mathrm{k\Omega}$, $R_2 = 10\,\mathrm{k\Omega}$, $C = 0.5\,\mu\mathrm{F}$, cutoff frequency = 32 Hz) and a high cutoff frequency condition ($R_1 = 2\,\mathrm{k\Omega}$, $R_2 = 10\,\mathrm{k\Omega}$, $C = 0.01\,\mu\mathrm{F}$, cutoff frequency = 1.6 kHz). The measurement frequency range was 0.1 Hz to 1 MHz.

The resulting Nyquist plots show that, regardless of the cutoff frequency of the RC circuit, Z_1 corresponds to a resistive component of 2 kΩ, while Z_2 appears as a semicircle corresponding to a parallel connection of a 10 kΩ resistor and a capacitor. These results demonstrate that the proposed SIM method enables acquisition of impedance spectra over a wide frequency range spanning seven orders of magnitude (0.1 Hz–1 MHz). Furthermore, the circuit parameters can be estimated from the obtained spectra.

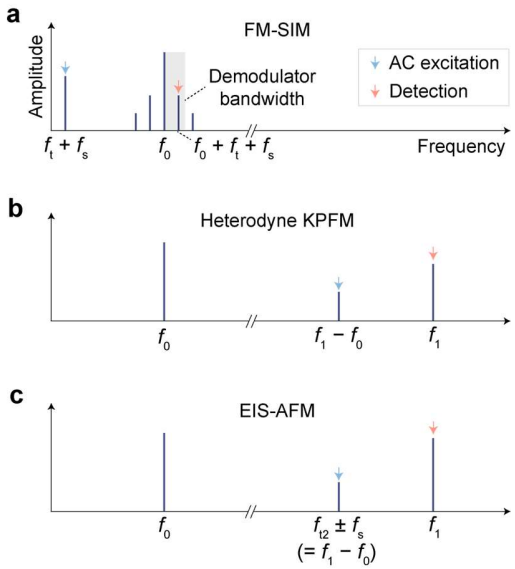

Supplementary Fig. 1 | Comparison of the cantilever frequency spectra for different measurement methods based on distinct electrostatic force detection schemes. **a**, Frequency modulation (FM) SIM. **b**, Heterodyne KPFM. **c**, EIS-AFM.

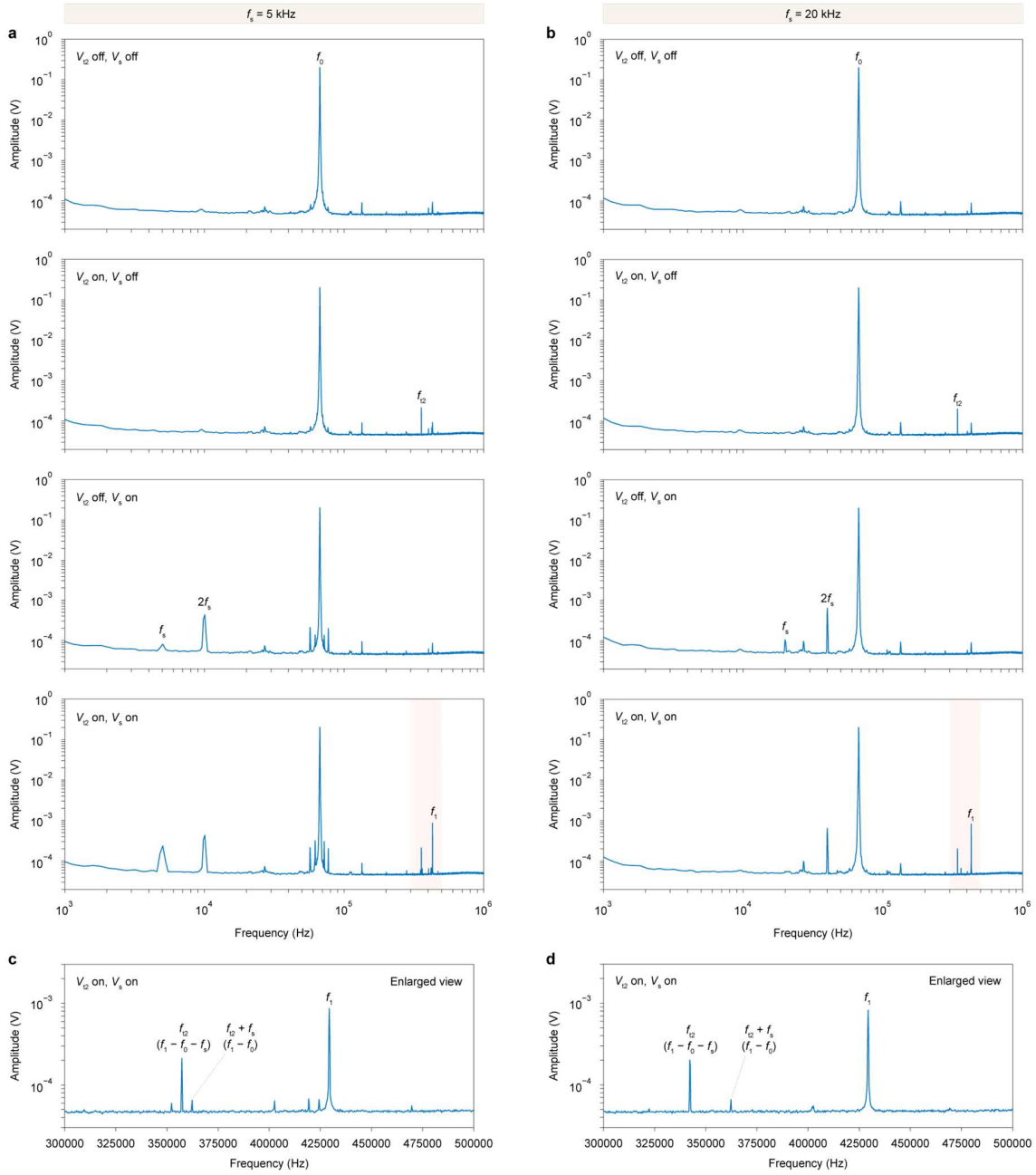

Supplementary Fig. 2 | Comparison of the cantilever vibration spectra obtained with different on/off combinations of the AC signals applied to the tip and sample. V_{t2} and V_s denote the amplitudes of the AC signals with frequencies f_{t2} and f_s applied to the tip and sample, respectively. **a,** Spectra for f_s = 5 kHz. **b,** Spectra for f_s = 20 kHz. **c-d,** Enlarged views of the spectra near the second resonance mode for the V_{t2} on, V_s on condition in **a** and **b**, respectively. To reduce unwanted peaks, the KPFM voltage feedback was held during the measurements, and the AC signal applied to the tip for KPFM was turned off.

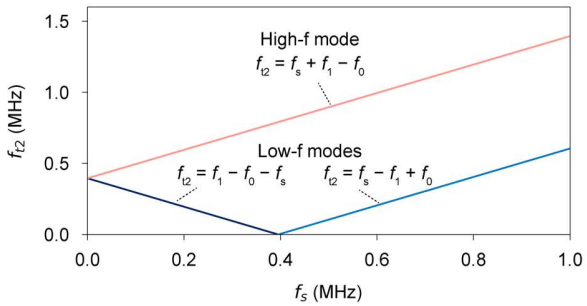

Supplementary Fig. 3 | Relationship between the frequencies of the AC signals applied to the sample and the probe in EIS-AFM. In the high-f mode, the frequencies follow a single relationship, although the required value of f_{t2} becomes large. In contrast, in the low-f modes, two relationships must be switched, but f_{t2} can be kept small. Unless otherwise noted, all measurements in this study were performed using the low-f modes.

164

165

166

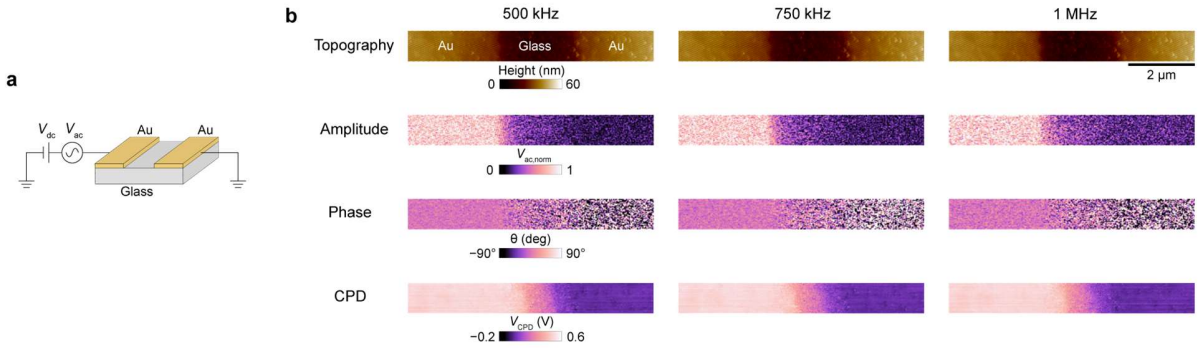

Supplementary Fig. 4 | High-frequency EIS-AFM measurement results using an Au electrode sample. a, Schematic illustration of the test measurement. **b**, SIM measurement results obtained when the frequency of the AC signal applied to the sample was set to 500 kHz, 750 kHz, and 1 MHz. The topography, SIM amplitude and phase, and CPD images obtained by KPFM are shown. The AC signal was applied to the Au electrode on the left side of the image.

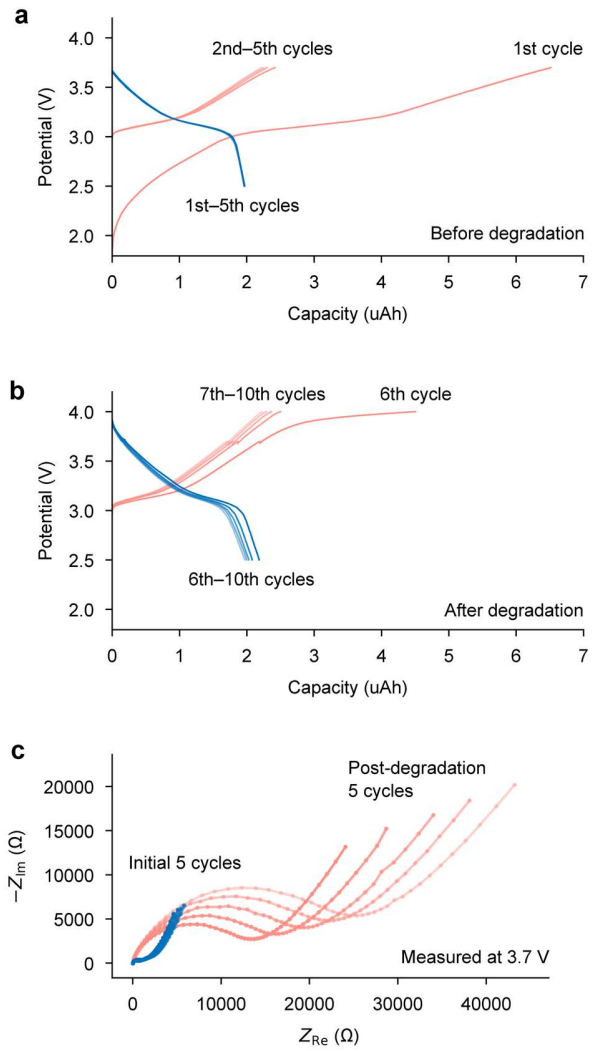

Supplementary Fig. 5 | High-voltage degradation of the NCM cathode cell. a, Charge–discharge curves for cycles 1–5. **b**, Charge–discharge curves for cycles 6–10 after increasing the charge cutoff voltage to 4 V (vs. InLi). **c**, Nyquist plots measured at each cycle. The cell potential during all EIS measurements was 3.7 V.

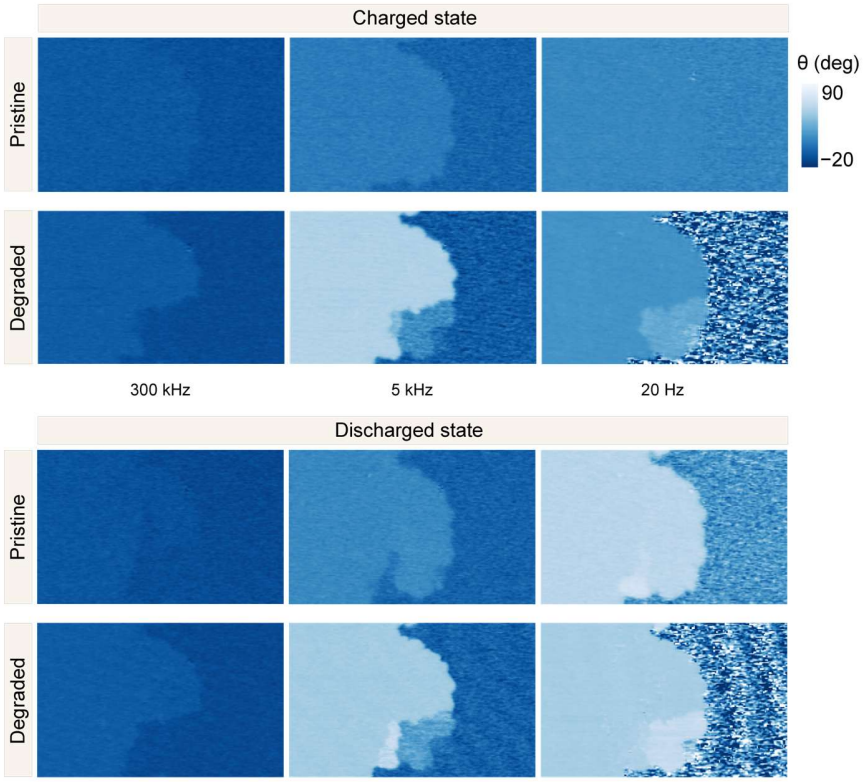

Supplementary Fig. 6 | Phase images from EIS-AFM measurements of high-voltage degradation near the NCM particle/sulfide SE interface. Results obtained at three frequencies (300 kHz, 5 kHz, and 20 Hz) are shown for both the charged and discharged states before and after high-voltage degradation.

173

174

175

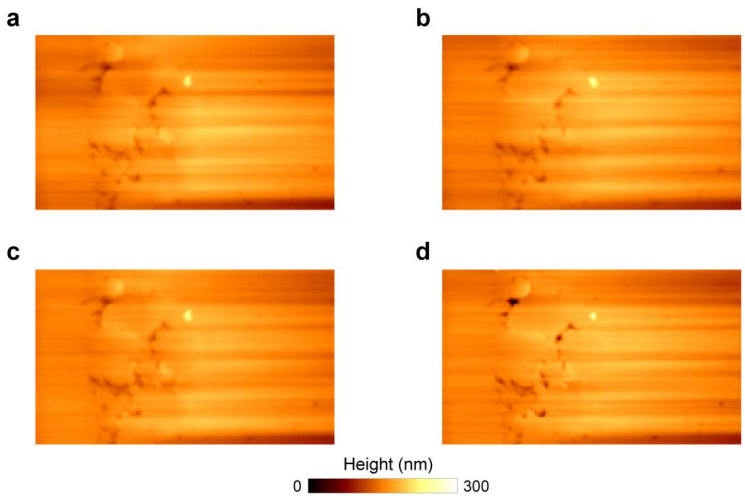

Supplementary Fig. 7 | Topographic images during a series of EIS-AFM measurements near the NCM cathode/sulfide SE interface. a, Charged state (3.4 V) before high-voltage degradation. **b**, Discharged state (2.5 V) before high-voltage degradation. **c**, Charged state after high-voltage degradation induced by holding the cell at 4.8 V (vs. Li/Li^+) for 24 h. **d**, Discharged state after the high-voltage degradation.

176

177

178

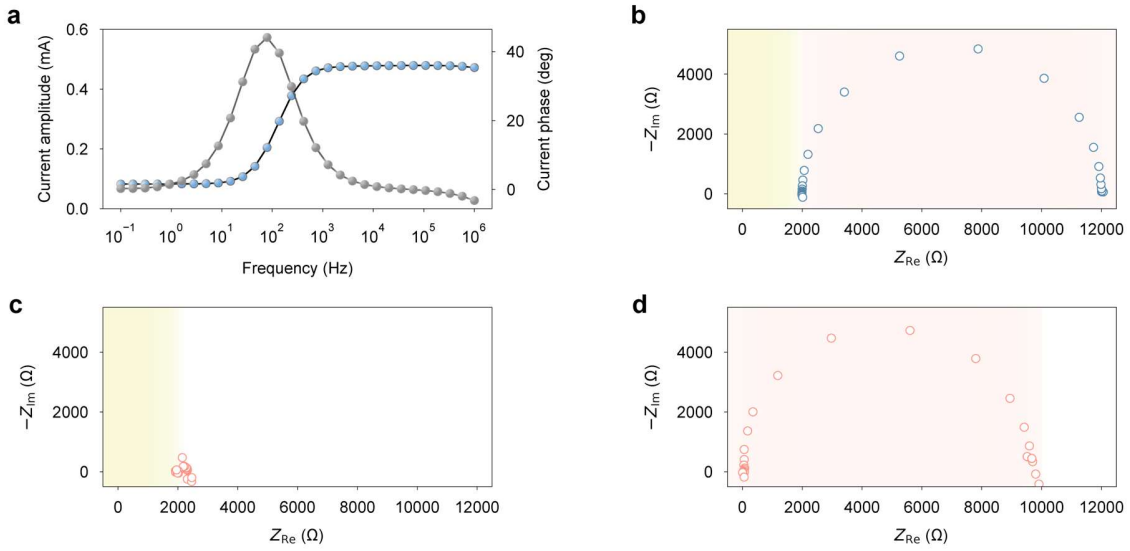

Supplementary Fig. 8 | Measurement of partial impedance spectra by EIS-AFM. a, Frequency spectra of the current amplitude and phase for the RC circuit used in the test measurement (R_1 = 2 kΩ, R_2 = 10 kΩ, C = 0.5 μF; cutoff frequency = 32 Hz). **b**, Nyquist plot of the total impedance of the entire circuit. **c-d**, Nyquist plots of the partial impedances (Z_1 and Z_2) of the RC circuit extracted from SIM measurement.

References

1. Kalinin, S. V. & Bonnell, D. A. Scanning impedance microscopy of electroactive interfaces. *Appl. Phys. Lett.* **78**, 1306–1308 (2001).

2. Kalinin, S. V. & Bonnell, D. A. Scanning impedance microscopy of an active Schottky barrier diode. *J. Appl. Phys.* **91**, 832–839 (2002).

3. Kimura, T., Kobayashi, K. & Yamada, H. Local impedance measurement of an electrode/single-pentacene-grain interface by frequency-modulation scanning impedance microscopy. *J. Appl. Phys.* **118**, 055501 (2015).

4. Sugawara, Y. *et al.* High potential sensitivity in heterodyne amplitude-modulation Kelvin probe force microscopy. *Appl. Phys. Lett.* **100**, 223104 (2012).

5. Ishida, N. Local impedance measurement by direct detection of oscillating electrostatic potential using Kelvin probe force microscopy. *Journal of Physical Chemistry C* **126**, 17627–17634 (2022).